


## Orbital-selective coherence-incoherence crossover and metal-insulator transition in Cu-doped NaFeAs

S. L. Skornyakov , V. I. Anisimov , and I. Leonov 

*M. N. Miheev Institute of Metal Physics of Ural Branch of Russian Academy of Sciences,  
18 S. Kovalevskaya Street, Yekaterinburg 620137, Russia  
and Ural Federal University, Yekaterinburg 620002, Russia*

 (Received 16 January 2021; revised 18 March 2021; accepted 29 March 2021; published 9 April 2021)

We study the effects of electron-electron interactions and hole doping on the electronic structure of Cu-doped NaFeAs using the density functional theory plus dynamical mean-field theory (DFT+DMFT) method. In particular, we employ an effective multiorbital Hubbard model with a realistic band structure of NaFeAs in which Cu-doping was modeled within a rigid band approximation and compute the evolution of the spectral properties, orbital-selective electronic mass renormalizations, and magnetic properties of NaFeAs on doping with Cu. In addition, we perform fully charge self-consistent DFT+DMFT calculations for the long-range antiferromagnetically ordered Na(Fe,Cu)As with Cu  $x = 0.5$  with a real-space ordering of Fe and Cu ions. Our results reveal a crucial importance of strong electron-electron correlations and local potential difference between the Cu and Fe ions for understanding the  $\mathbf{k}$ -resolved spectra of Na(Fe,Cu)As. On Cu-doping, we observe a strong orbital-selective localization of the Fe  $3d$  states accompanied by a large renormalization of the Fe  $xy$  and  $xz/yz$  orbitals. Na(Fe,Cu)As exhibits bad-metal behavior associated with a coherence-to-incoherence crossover of the Fe  $3d$  electronic states and local moments formation near a Mott metal-insulator transition (MIT). For heavily doped NaFeAs with Cu  $x \sim 0.5$  we obtain a Mott insulator with a band gap of  $\sim 0.3$  eV which is characterized by divergence of the quasiparticle effective mass of the Fe  $xy$  states. In contrast to this, the quasiparticle weights of the Fe  $xz/yz$  and  $e$  states remain finite at the MIT. The MIT occurs via an orbital-selective Mott phase to appear at Cu  $x \simeq 0.375$  with the Fe  $xy$  states being Mott localized. We propose the possible importance of Fe/Cu disorder to explain the magnetic properties of Cu-doped NaFeAs.

DOI: [10.1103/PhysRevB.103.155115](https://doi.org/10.1103/PhysRevB.103.155115)

### I. INTRODUCTION

The discovery of unconventional superconductivity in high- $T_c$  cuprates and in Fe-based pnictides and chalcogenides (Fe-based superconductors, FeSCs) has received enormous attention over the past several decades [1–3]. The high- $T_c$  cuprates and FeSCs show many similarities, e.g., in the vast class of FeSCs and cuprates, superconductivity appears as a result of the suppression of a long-range, antiferromagnetic (AFM) or nematic phase [1–4]. It has been proposed that AFM spin fluctuations play a decisive role in the mechanism of the  $s^\pm$  (in FeSCs) and  $d$ -wave (in cuprates) high- $T_c$  superconductivity [1–8]. In addition, both FeSCs and cuprates reveal the crucial importance of strong correlations that favor electronic localization and severe orbital-selective quasiparticle mass renormalizations [9–15].

At the same time, the electronic properties of the parent phases of FeSCs and cuprate superconductors are significantly different. In fact, the parent phase of cuprates is a Mott (or charge transfer) insulator with localized magnetic moments [1,3,16]. Its doping leads to a Mott insulator-metal transition which is followed by the emergence of high- $T_c$  superconductivity. In contrast, FeSCs are bad metals in their parent phase [2,3,9,11–14]. This suggests an intermediate range of correlation strength in FeSCs and seems to point out the

itinerant nature of their magnetic moments. The latter has been attributed to the multiorbital character of the electronic structure of FeSCs, in stark contrast to the one-band behavior of cuprates. Although bad-metal behavior and large band renormalizations in FeSCs can in principle be explained by the proximity to an orbital-selective Mott phase, no correlated insulating state has been reported in FeSCs despite significant research efforts [13,14,17]. For quite a long time it was unclear whether or not a correlated (Mott or charge transfer) insulator can be realized in the phase diagram of FeSCs.

In order to address this question, Song *et al.* conducted a detailed experimental study of the iron pnictide NaFeAs doped with Cu [18]. It was established that the heavily doped Na(Fe $_{1-x}$ Cu $_x$ )As with  $x \sim 0.5$  exhibits a real-space ordering of Fe and Cu ions and makes a phase transition in a Mott-insulating state. Na(Fe $_{1-x}$ Cu $_x$ )As with  $x \sim 0.5$  exhibits insulating behavior in the dc resistivity up to room temperature with an activation energy of  $\sim 100$  meV [18–20]. Below the Néel temperature  $T_N \simeq 200$  K the insulating phase concurs with a long-range AFM  $(1, 0, \frac{1}{2})$  ordering. The insulating behavior was found to persist well above  $T_N$ , implying that Na(Fe,Cu)As with Cu  $x \simeq 0.5$  is a Mott insulator, in accordance with scanning tunneling microscopy measurements near  $x = 0.3$  [21]. Moreover, consistent with a more local origin of magnetism in Na(Fe,Cu)As with  $x \simeq 0.5$ , the ordered

magnetic moment of Fe ions in AFM NaFe<sub>0.5</sub>Cu<sub>0.5</sub>As  $\sim 1.1 \mu_B$  is sufficiently higher than that in the spin-density wave AFM phase of undoped NaFeAs,  $\sim 0.09\text{--}0.32 \mu_B$  [22–24]. It is also interesting to note that the Néel temperature in NaFeAs (Cu  $x = 0$ ) is relatively small,  $T_N \sim 40$  K [23–25]. In fact, it is significantly smaller than that in the heavily Cu-doped NaFeAs ( $\sim 200$  K), implying the rise of magnetic correlations in NaFeAs on Cu-doping.

Most notably, on decreasing  $x$  from 0.5, the value of the ordered magnetic moment was found to gradually decrease until bulk superconductivity emerges below  $x \sim 0.05$ , with a critical temperature  $T_c \simeq 11$  K [19,26]. In this respect, Na(Fe<sub>1-x</sub>Cu<sub>x</sub>)As is a unique system among FeSCs in which superconductivity seems to be “smoothly” connected to a Mott-insulating state, implying the importance of electron correlations for sustaining of the high- $T_c$  superconductivity in FeSCs. In addition, angle-resolved photoemission (ARPES) measurements combined with the electronic band structure calculations within the DFT+ $U$  method have shown that at  $x \sim 0.44$ , Na(Fe<sub>1-x</sub>Cu<sub>x</sub>)As is a narrow-gap insulator with the energy gap originating from the on-site Coulomb interactions of the Fe 3*d* orbitals [20,27]. This behavior has been confirmed by the DFT+dynamical mean-field theory (DFT+DMFT) [28] analysis given by Charnukha *et al.* [29]. In particular, it was shown that mutual agreement between the theoretical and the experimental ARPES spectra can be significantly improved by taking into account the dynamical on-site Coulomb correlations within DFT+DMFT. Based on a detailed comparison of optical spectroscopy and DFT+DMFT results, the authors proposed that Na(Fe,Cu)As is a correlated Slater insulator, characterized by the crossover from a correlated-insulator to metal phase with highly incoherent charge transport due to large fluctuating moments. Moreover, nuclear magnetic resonance measurements of the magnetic phase of Na(Fe,Cu)As for  $x \leq 0.5$  performed by Xin *et al.* reveal the possible existence of defects of the Fe and Cu stripes in Na(Fe,Cu)As [30]. This result suggests that the electronic state of Na(Fe<sub>1-x</sub>Cu<sub>x</sub>)As can also be affected by Cu/Fe disorder which plays as an extra mechanism promoting the correlated insulating state at  $x \sim 0.5$ . Overall, these results demonstrate that electronic correlation effects in the Fe 3*d* states are an essential ingredient for understanding the electronic structure of Na(Fe,Cu)As.

Applications of DFT+DMFT have proven to give a good quantitative description of the electronic structure and magnetic properties of various FeSCs, including NaFeAs [9–15,17,28,29,31,32]. However, these investigations mostly deal with the electronic structure and magnetic properties of FeSCs in their normal metallic state, while the studies of a Mott-insulating phase in the phase diagram of FeSCs are still open to debate. In our work, we explore the effects of electron-electron interactions and hole doping (substitution of Fe with Cu) on the electronic structure and magnetic properties of Cu-doped NaFeAs using the DFT+DMFT method [28]. We employ an effective multiorbital Hubbard model with a realistic band structure of NaFeAs in which Cu-doping was modeled using a rigid band approximation. We use DMFT to compute the evolution of the spectral properties, orbital-dependent quasiparticle band renormalizations  $m^*/m$ , local spin susceptibilities, and symmetry of spin fluctuations of

NaFeAs on doping with Cu. In addition, we perform the fully self-consistent DFT+DMFT calculations for the long-range antiferromagnetically ordered Na(Fe,Cu)As with Cu  $x = 0.5$ . In this calculation we consider NaFe<sub>0.5</sub>Cu<sub>0.5</sub>As supercell with real-space ordering of Fe and Cu ions as determined from x-ray diffraction [18]. Our results reveal a crucial importance of strong electron-electron correlations and local potential difference between the Cu and Fe ions in Na(Fe,Cu)As. On Cu-doping, we observe a strong orbital-selective localization of the Fe 3*d* states accompanied by a large renormalization of the Fe *xy* and *xz/yz* orbitals. Na(Fe,Cu)As shows bad-metal behavior associated with a coherence-to-incoherence crossover of the Fe 3*d* electronic states and local moments formation. For Cu  $x > 0.375$  it undergoes a Mott-Hubbard metal-insulator transition. It is found to occur via an intermediate orbital-selective Mott phase to appear at Cu  $x \simeq 0.375$ , in which the Fe 3*d xy* orbital is Mott localized while other Fe 3*d* orbitals are metallic [11]. Moreover, our results suggest the possible importance of Fe/Cu disorder to explain the magnetic properties of Cu-doped NaFeAs.

## II. RESULTS AND DISCUSSION

### A. Model approach to paramagnetic Na(Fe,Cu)As

We start our theoretical analysis of the effects of electron correlations and Cu-doping on the electronic structure of paramagnetic (PM) Na(Fe,Cu)As by constructing a multiorbital Hubbard model for stoichiometric NaFeAs (Cu  $x = 0$ ). For this purpose, we built up a model tight-binding Hamiltonian which explicitly includes the Fe 3*d* and As 4*p* valence states employing atomic-centered Wannier functions constructed within the energy window spanned by the Fe 3*d* and As 4*p* valence states of NaFeAs [33]. For the Fe 3*d* states, the tight-binding Hamiltonian is supplemented by the on-site Coulomb interaction  $U = 3.5$  eV and Hund’s exchange coupling  $J = 0.85$  eV. These values are typical for FeSCs according to different estimations [31]. In our calculations, we employ the DFT+DMFT method [34–36] implemented within the plane-wave pseudopotential formalism with a gradient-corrected approximation in DFT [37].

For Cu-doping  $x = 0$  the calculated within DFT the Wannier Fe 3*d* electron density is about 7.35 (per Fe ion). To model the effects of Cu-doping on the electronic structure of Na(Fe,Cu)As, we apply a rigid-band shift of the Fermi level within DFT. We note that in such an approach the effects of a local potential difference between Cu and Fe are not taken into account. We consider them explicitly in the supercell DFT+DMFT calculations for Cu  $x = 0.5$ ; see Sec. II B. In fact, Cu  $x = 0.5$  corresponds to the hole doping by two electrons of the unit cell containing two formula units of NaFeAs. The DMFT many-body problem was solved using the hybridization expansion continuous-time (segment) quantum Monte Carlo method [38]. The Coulomb interaction was treated in the density-density form neglecting the effects of spin-orbit coupling. We use the fully localized double-counting correction, evaluated from the self-consistently determined local occupations, to account for the interactions already described by DFT. The angle-resolved spectra were evaluated from

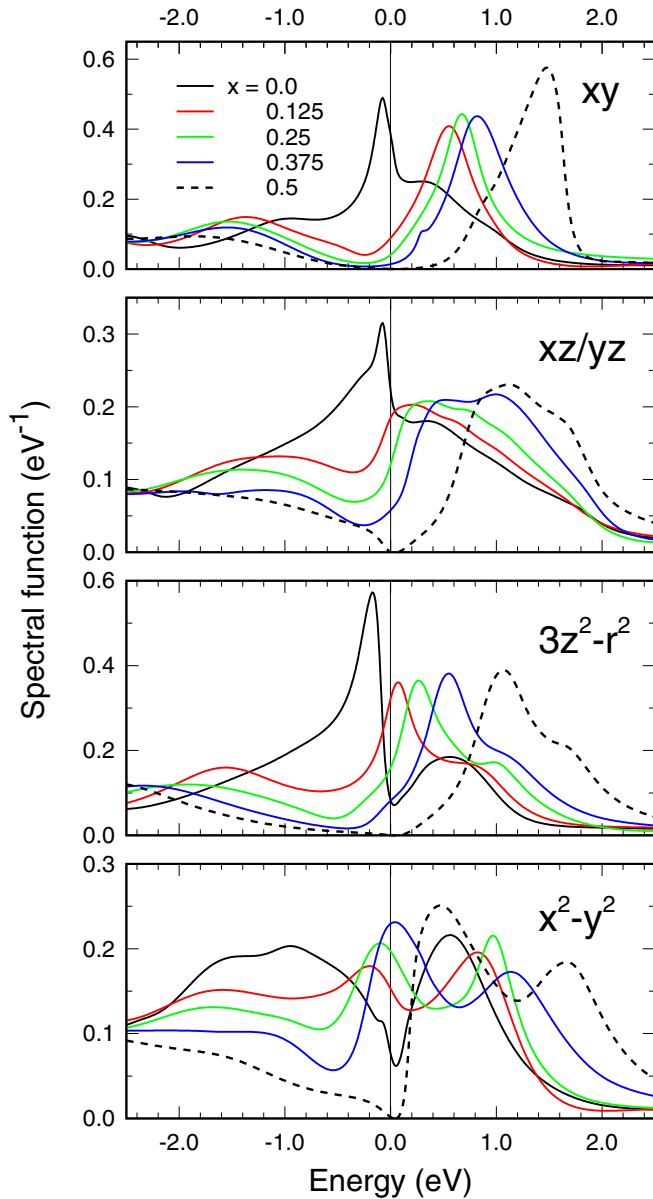


FIG. 1. Orbitally resolved Fe-3d spectral functions of a tight-binding model of PM Na(Fe,Cu)As for various Cu  $x$  obtained within DMFT at  $T = 290$  K.

analytic continuation of the self-energy results using Padé approximants [39].

We begin with an evaluation of the electronic structure of PM Na(Fe,Cu)As. In Fig. 1 we display our results for the Fe 3d spectral functions computed by DMFT for the model Hamiltonian of Na(Fe,Cu)As on different Cu  $x$  from 0 to 0.5 (hole doping from 0 to 2.0). Our results for the  $\mathbf{k}$ -resolved spectral functions calculated within DMFT along the  $\Gamma$ -X-M- $\Gamma$  path in the Brillouin zone (BZ) are shown in Fig. 2. In agreement with previous results, for  $x = 0$  DMFT yields a correlated metal with the electronic structure being typical for FeSCs. In particular, the Fe 3d states are  $\sim 4$  eV wide and show a sharp peak below the Fermi level due to the Van Hove singularity of the Fe  $xy$  and  $xz/yz$  orbitals at the BZ M-point. Our results for the Fermi surface are similar

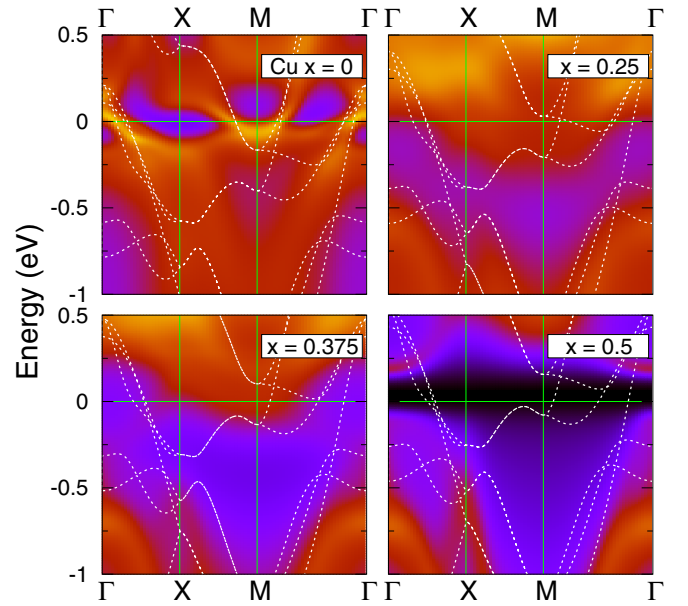


FIG. 2. Electronic structure of a tight-binding model for PM Na(Fe,Cu)As along the  $\Gamma$ -X-M- $\Gamma$  path in the BZ for different Cu  $x$  calculated by DFT+DMFT at  $T = 290$  K (contours) and DFT (dashed curves).

to those in FeSCs, with two elliptic electron pockets near the M point (due to the Fe  $xz/yz$  and  $xy$  bands) and two nearly degenerate circular hole pockets at the  $\Gamma$  point. We note that for  $x = 0$  our DMFT results for the Fermi surface are qualitatively similar to those obtained by DFT. In addition, we observe a remarkable orbital-selective renormalization of the Fe 3d bands, resulting in a sizable shift (in comparison to the DFT result) of the Van Hove singularity of the Fe  $t_2$  ( $xy$  and  $xz/yz$ ) bands at the BZ M-point toward the Fermi level. In fact, our analysis of the orbitally resolved quasiparticle mass enhancement evaluated as  $m^*/m = 1 - \partial \text{Im} \Sigma(\omega) / \partial \omega |_{\omega=0}$  using Padé extrapolation of the self-energy  $\Sigma(\omega)$  to  $\omega \rightarrow 0$  on the imaginary axis yields  $m^*/m \sim 4.3$  and 3.5 for the Fe  $xy$  and  $xz/yz$  orbitals (see Table I). The effective mass of the Fe  $x^2 - y^2$  and  $3z^2 - r^2$  orbitals reveals a weaker renormalization of  $\sim 2.2$ –2.6.

On hole doping our nonmagnetic DFT results show a smooth shift of the Fermi level of NaFeAs. Thus, for Cu  $x = 0.5$  it shifts by  $\sim 330$  meV (see Fig. 2). For Cu  $x = 0.5$  DFT gives a metal, in contrast to a Mott-insulating behavior determined in the experiments (as it is expected due to the neglect of the effect of correlations). This suggests the

TABLE I. Orbitally resolved quasiparticle band mass enhancement  $m^*/m$  in the tight-binding model of PM Na(Fe,Cu)As computed by DMFT at different hole dopings and  $T = 290$  K.

Cu $x$	$3z^2 - r^2$	$xz/yz$	$xy$	$x^2 - y^2$
0.0	2.60	3.49	4.34	2.16
0.125	3.31	3.06	5.68	2.03
0.25	3.43	4.95	8.29	2.27
0.375	3.46	6.14	9.60	2.83

crucial importance of electronic correlations of the Fe 3d states in NaFeAs. In agreement with this, using DMFT we obtain a large spectral weight transfer from low to high energies on Cu-doping, which is accompanied by a metal-to-insulator phase transition for Cu  $x > 0.375$ . It is accompanied by a remarkable shift of the Fe 3d spectral function peaks across the Fermi level,  $E_F$  (see Fig. 1). In particular, the peaks due to the  $xy$  and  $xz/yz$  orbitals shift above  $E_F$  for Cu  $x > 0.125$ , while for the  $x^2 - y^2$  it is at about  $x \sim 0.375$ . In the same time, the spectral function of the  $x^2 - y^2$  orbital reveals different behavior on Cu-doping. Unlike the Fe  $t_2$  and  $3z^2 - r^2$  orbitals, it shows two peaks below and above  $E_F$ , shifting to the higher energies.

Most notably, for Cu  $x > 0.375$  we observe a sharp reconstruction of the electronic structure of PM Na(Fe,Cu)As, associated with a Mott metal-insulator transition (MIT), in agreement with experiment [18,20]. Our results reveal a remarkable orbital selectivity in Na(Fe,Cu)As. Thus, for Cu  $x = 0.375$  the most heavily renormalized Fe  $xy$  orbital is seen to be insulating (Mott localized), whereas other Fe 3d orbitals are still metallic (itinerant), which is indicative of an orbital-selective Mott phase [11]. We obtain that Na(Fe,Cu)As with Cu  $x = 0.5$  is a Mott insulator with a  $d-d$  energy gap of 0.2 eV. We note that this result agrees well with the previous model DMFT calculations based on a slave-spin approach which also found a Mott insulator in the absence of a long-range AFM order in heavily Cu-doped NaFeAs [40]. At the same time, we observe a sizable difference in the  $\mathbf{k}$ -resolved spectral function of Na(Fe,Cu)As as compared to the ARPES measurements [20]. It is presumably due to the absence of the effects of a local potential difference between the Cu and Fe ions in our model DMFT calculations. We note that using different Hubbard  $U$  and Hund's coupling  $J$  does not improve the  $\mathbf{k}$ -resolved spectral functions of Na(Fe,Cu)As.

The Mott transition is accompanied by strong orbital-selective localization of the Fe 3d electrons [11]. In fact, we obtain a large orbital-dependent enhancement of the effective mass of the Fe 3d states on Cu-doping as shown in Table I. In particular, at the verge of a Mott transition, at Cu  $x = 0.375$ ,  $m^*/m$  is about 9.6 and 6.1 for the Fe  $xy$  and  $xz/yz$  bands, respectively. For the  $e$  states the mass renormalizations are significantly weaker,  $m^*/m \sim 2.8$  and 3.5 for the  $x^2 - y^2$  and  $3z^2 - r^2$  orbitals, respectively. This result points out that the planar  $xy$  orbital is most renormalized, consistent with the appearance of an orbitally selective Mott state [7,13]. Moreover, our results suggest that the quasiparticle effective mass  $m^*/m$  of the Fe  $xy$  states diverges [i.e.,  $\text{Im}\Sigma(\omega)$  diverges for  $\omega \rightarrow 0$ ] at the metal-insulator transition in Na(Fe,Cu)As [34,41]. In contrast to this the  $xz/yz$  and  $e$  quasiparticle weights remain finite at the MIT. This implies the crucial importance of strong orbital-selective correlations of the Fe 3d states to determine the electronic and magnetic properties of heavily Cu-doped NaFeAs.

On hole doping, we observe a significant enhancement of incoherence of the spectral weight of the Fe 3d states, suggesting a bad-metallic behavior of Na(Fe,Cu)As associated with the proximity to a Mott transition [9,11,16]. This behavior is accompanied by a doping-induced local moments formation in Na(Fe,Cu)As which results in a significant growth of the

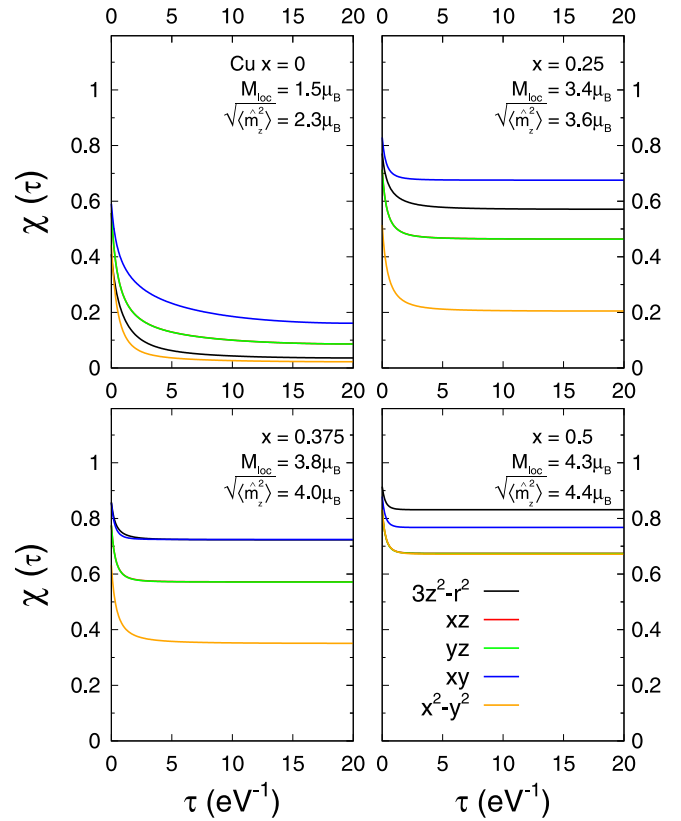


FIG. 3. Orbitaly resolved local spin susceptibility  $\chi(\tau)$ , instantaneous  $\sqrt{\langle \hat{m}_z^2 \rangle}$ , and fluctuating  $M_{\text{loc}}$  magnetic moments of a tight-binding model for PM Na(Fe,Cu)As computed at different Cu  $x$  by DFT+DMFT at  $T = 290$  K.

fluctuating local magnetic moments. In fact, on an increase of Cu-doping  $x$  from 0 to 0.5 the instantaneous local magnetic moments  $\sqrt{\langle \hat{m}_z^2 \rangle}$  vary from 2.3 to 4.4  $\mu_B$  (the corresponding fluctuating moments  $M_{\text{loc}}$  evaluated as the imaginary-time average of the local spin susceptibility  $\chi(\tau) = \langle \hat{m}_z(\tau) \hat{m}_z(0) \rangle$  as  $M_{\text{loc}} = [T \int \chi(\tau) d\tau]^{1/2}$  are 1.5 and 4.3  $\mu_B$ , respectively). We therefore conclude that the transition is accompanied by a crossover from itinerant to localized moment behavior of the Fe 3d states. The latter is seen from our results for the orbitaly resolved contributions to  $\chi(\tau)$  computed by DMFT for different hole doping (see Fig. 3). Indeed, on doping the Fe 3d electrons tend to localize to form fluctuating moments:  $\chi(\tau)$  is seen to be almost constant, independent of  $\tau$  and close to its maximal value. Our results also reveal strong orbital dependence of the local moments on hole doping, with the  $xy$  and  $3z^2 - r^2$  orbitals being most localized at high doping level.

It is interesting to note that on doping (in the metallic phase) we observe a remarkable reconstruction of the electronic band structure of Na(Fe,Cu)As, associated with a change of the Fermi surface topology. It is accompanied by a reconstruction of magnetic correlations which can be approximately estimated by using the momentum-dependent static spin susceptibility  $\chi(\mathbf{q})$ . Our result for  $\chi(\mathbf{q})$  at  $x = 0$  evaluated using the particle-hole bubble approximation shows a maximum at the BZ M-point (see Fig. 4), which is characterized by an in-plane nesting wave vector  $(\pi, \pi)$ , consistent

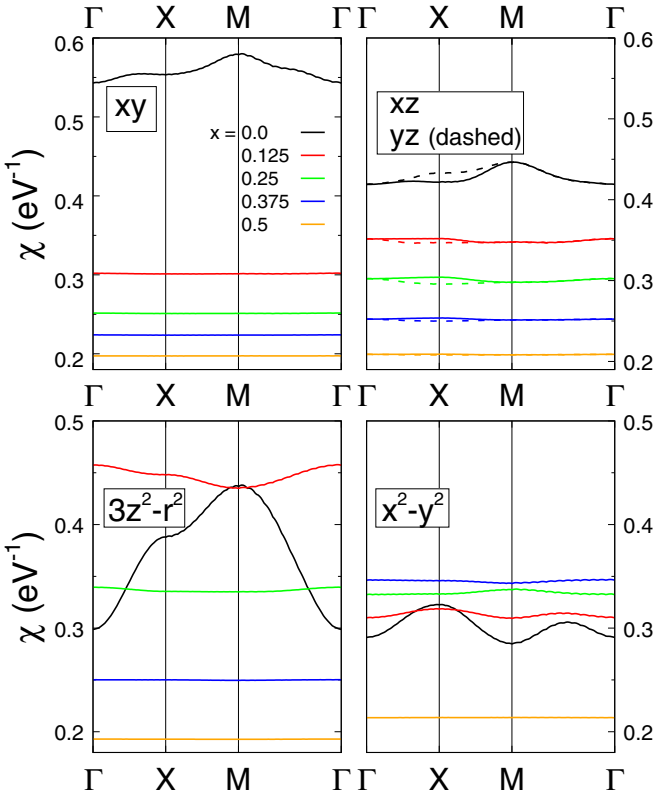


FIG. 4. Orbitaly resolved static spin susceptibility  $\chi(\mathbf{q})$  of a tight-binding model for PM Na(Fe,Cu)As along the  $\Gamma$ -X-M- $\Gamma$  path as a function of Cu-doping  $x$  computed by DFT+DMFT at  $T = 290$  K.

with  $s^\pm$  pairing symmetry in FeSCs [5–7]. This confirms that the leading magnetic instability of pure NaFeAs at ambient pressure occurs at the wave vector  $(\pi, \pi)$ , consistent with the spin excitation spectra of FeSCs [42]. On doping we observe a smooth decrease of  $\chi(\mathbf{q})$  for the  $t_2$  orbitals which becomes almost flat and featureless already at  $x = 0.125$ . In contrast, the shape of the  $e$  orbitals susceptibility shows a less trivial doping dependence; at  $x = 0.125$   $\chi(\mathbf{q})$  for the  $3z^2 - r^2$  states exhibits a sharp damping of the peak at the M point which is accompanied by a slight increase of ferromagnetic fluctuations.  $\chi(\mathbf{q})$  for the  $x^2 - y^2$  states displays a flattening and a uniform increase followed by a sharp drop on the verge of the Mott transition.

Overall, our results imply strong localization of the  $3d$  electrons on a doping-induced MIT in Na(Fe,Cu)As. On Cu-doping from  $x = 0$  to 0.5, Na(Fe,Cu)As shows a remarkable reconstruction of the electronic structure and coherence-to-incoherence crossover of the Fe  $3d$  electronic states, associated with a Mott transition and the effect of local moments formation near the MIT. This implies the crucial importance of strong correlations that favor electronic localization and strong orbital-selective quasiparticle mass enhancement in Na(Fe,Cu)As near the Mott-insulating phase [9,11,13,14]. While the above DMFT calculations do not consider the effects of a local potential difference between the Cu and the Fe ions, these results demonstrate that electron correlations in the Fe  $3d$  states are an essen-

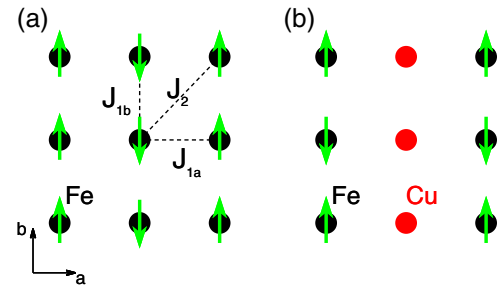


FIG. 5. In-plane static magnetic configurations of (a) stoichiometric NaFeAs and (b) Cu-doped NaFe<sub>0.5</sub>Cu<sub>0.5</sub>As used in the DFT+DMFT calculations. The dashed lines show dominating exchange paths.

tial ingredient for understanding the electronic properties of Na(Fe,Cu)As.

### B. DFT+DMFT calculations of AFM NaFe<sub>0.5</sub>Cu<sub>0.5</sub>As

Next, we perform a realistic DFT+DMFT study of the electronic structure and magnetic properties of Na(Fe<sub>1-x</sub>Cu<sub>x</sub>)As with the real-space stripe-type ordering of the Fe and Cu ions as found experimentally near  $x = 0.5$  (see Fig. 5). In our calculations, we employ the state-of-the-art fully self-consistent in charge density DFT+DMFT method implemented within the plane-wave pseudopotential formalism [34–36]. In our DFT+DMFT calculations we explicitly include the Fe  $3d$ , As  $4p$ , and Cu  $3d$  states for the Cu  $x = 0.5$  doped Na(Fe,Cu)As by constructing a basis set of atomic-centered Wannier functions within the energy window spanned by these bands [33]. This allows us to take into account a charge transfer between the partially occupied  $3d$  and  $4p$  states, accompanied by the strong on-site Coulomb correlations of the Fe  $3d$  electrons. The Cu  $3d$  states are nearly fully occupied with a Cu<sup>1+</sup> $3d^{10}$  configuration and therefore in our DFT+DMFT calculations, we do not consider subtle correlations effects in the Cu  $3d$  states. We use the same Hubbard  $U = 3.5$  eV and Hund’s rule coupling  $J = 0.85$  eV for the Fe  $3d$  states as those in the model calculation (see Sec. II A). In DFT+DMFT, the quantum impurity problem was solved using the continuous time quantum Monte Carlo (segment) method [38]. The fully localized double-counting correction, evaluated from the self-consistently determined local occupations, was employed. The DFT+DMFT calculations are performed for an antiferromagnetically ordered state of Na(Fe,Cu)As at a temperature  $T \sim 290$  K. We use the experimentally established stripe configuration of the in-plane Fe moments as shown in Fig. 5 [18]. Note that the AFM structure of the Cu-doped compound is obtained from that of NaFeAs by replacing the ferromagnetic stripes by Cu ions. In our spin-polarized DFT+DMFT calculations, we employ the spin-polarized DFT. Moreover, we explore the effect of Cu-doping on the magnetic properties of Na(Fe,Cu)As by computing the exchange couplings of the Heisenberg model within spin-polarized DFT+DMFT using the magnetic force theorem [43].

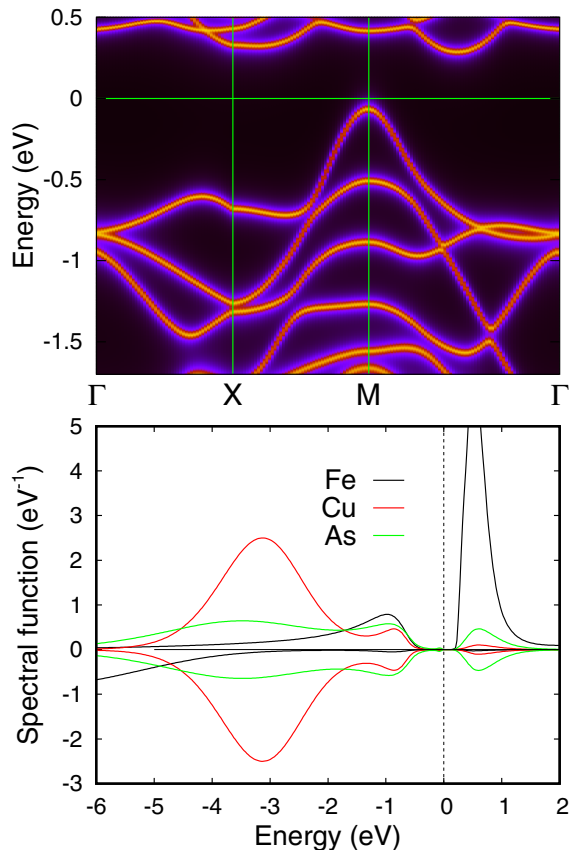


FIG. 6. Electronic structure along the  $\Gamma$ -X-M- $\Gamma$  path (upper panel) and spin-resolved atomic-projected spectral functions of AFM  $\text{NaFe}_{0.5}\text{Cu}_{0.5}\text{As}$  as obtained by DFT+DMFT at  $T = 290$  K.

We perform spin-polarized DFT+DMFT calculations of the spectral properties of  $\text{Na}(\text{Fe,Cu})\text{As}$  with  $\text{Cu } x = 0.5$ . Our results for the orbitally resolved Fe  $3d$ , Cu  $3d$ , and As  $4p$  spectra are shown in Fig. 6 along with the  $\mathbf{k}$ -resolved spectral functions of AFM  $\text{NaFe}_{0.5}\text{Cu}_{0.5}\text{As}$  obtained by DFT+DMFT. Our results exhibit a correlated insulator behavior with a band gap of  $\sim 0.3$  eV, in agreement with experiments and previous theoretical estimates [18,20]. It is interesting to note high coherence of the electronic states of AFM  $\text{NaFe}_{0.5}\text{Cu}_{0.5}\text{As}$  to that in the PM phase (see Fig. 2), consistent with previous studies [29,44]. Our result for the local magnetic moment of about  $3.65 \mu_B$  (fluctuating moment  $3.46 \mu_B$ ) is compatible with that in our model DMFT calculations for Cu-doping  $x = 0.5$ . The spectral function of  $\text{Na}(\text{Fe,Cu})\text{As}$  with  $\text{Cu } x = 0.5$  shows a pronounced  $\sim 5$ – $6$  eV splitting of the Fe  $3d$  spin-up and spin-down states due to the magnetic exchange. Moreover, the spin-polarized DFT+DMFT calculations give a large ordered magnetic moment of  $3.61 \mu_B$  per Fe site. We note that this value of the ordered magnetic moment is significantly larger than that reported from neutron scattering,  $1.1 \mu_B/\text{Fe}$ , suggesting the crucial role of the nonlocal correlation effects and Cu/Fe disorder in  $\text{Na}(\text{Fe,Cu})\text{As}$  [45]. Our results highlight the key role of electronic correlations while AFM order alone within DFT could not open a gap in the electronic structure of  $\text{NaFe}_{0.5}\text{Cu}_{0.5}\text{As}$ . In addition, in DFT we observe that the overall bandwidth of heavily Cu-doped NaFeAs is decreased

from that in stoichiometric NaFeAs by  $\sim 20\%$ , triggering a MIT, in agreement with previous estimates [18].

By taking into account both the local potential difference between the Cu and Fe ions and on-site Coulomb correlations we obtain a much better agreement between the  $\mathbf{k}$ -resolved spectral function of  $\text{Na}(\text{Fe,Cu})\text{As}$  with  $x = 0.5$  and ARPES [20] compared to the model Hamiltonian results in Sec. II A. In particular, the spectral weight at the  $\Gamma$  point forms a weakly dispersive band in the energy interval from  $-0.5$  to  $-0.7$  eV along the  $\Gamma$ -X direction, in agreement with ARPES measurements [20]. We also observe a dispersive convex band along the X-M- $\Gamma$  line at the top of the valence band, which was absent in the model DMFT result for PM  $\text{Na}(\text{Fe,Cu})\text{As}$ .

We find a remarkable sensitivity of the electronic structure and magnetic correlations in NaFeAs with respect to doping with Cu. In Fig. 5 we display the in-plane magnetic states and exchange couplings of AFM  $\text{NaFe}_{1-x}\text{Cu}_x\text{As}$  for Cu  $x = 0$  and  $0.5$ . Our results for magnetic exchange couplings obtained from the spin-polarized DFT+DMFT magnetic force theorem calculations (for the Wannier Fe  $3d$  states) show a relatively large AFM intersite exchange coupling  $J_{1a} \sim 23$  meV (assuming an effective  $S = 2$  state per Fe ion) in AFM  $\text{NaFe}_{0.5}\text{Cu}_{0.5}\text{As}$  at a temperature 290 K [43,46]. Our results for the exchange couplings in AFM NaFeAs (Cu  $x = 0$ ) are  $J_{1a} = 31$  meV and  $J_{1b} = -22$  meV for the nearest neighbor and  $J_2 = 11$  meV for the next-nearest neighbor (here we assume a  $S = 1/2$  state) as obtained by the spin-polarized DFT+DMFT at  $T = 145$  K. This result agrees well with that obtained by more profound spin-wave calculations [25,47]. The calculated local and ordered magnetic moments in AFM NaFeAs are  $2.03$  and  $0.77 \mu_B/\text{Fe}$ , respectively. Moreover, in stoichiometric NaFeAs, the DFT+DMFT magnetization is found to sharply collapse to the PM state at temperatures above  $\sim 145$  K. Our results therefore suggest an intermediate range of correlation strength pointing out to itinerant nature of magnetic moments in pure NaFeAs.

### III. CONCLUSION

In conclusion, using DFT+DMFT we explored the effects of Coulomb correlations and hole doping on the electronic structure and magnetic properties of Cu-doped NaFeAs. On Cu-doping, we observe a strong orbital-dependent localization of the Fe  $3d$  states accompanied by a large renormalization of electronic mass of the Fe  $xy$  and  $xz/yz$  states.  $\text{Na}(\text{Fe,Cu})\text{As}$  shows bad-metal behavior associated with a coherence-to-incoherence crossover of the Fe  $3d$  electronic states and local moments formation near the MIT. For Cu  $x > 0.375$  it is found to undergo a Mott-Hubbard metal-insulator transition which is accompanied by divergence of the quasiparticle effective mass of the Fe  $xy$  states. In contrast to this, the  $xz/yz$  and  $e$  quasiparticle weights remain finite at the MIT. The Mott transition occurs via an intermediate orbital-selective Mott phase to appear at Cu  $x \simeq 0.375$  which is characterized by the Mott-localized Fe  $xy$  orbitals. Our DFT+DMFT results suggest a crucial importance of electron-electron correlations and local potential difference between the Cu and Fe ions in  $\text{Na}(\text{Fe,Cu})\text{As}$ . We propose a possible importance of Fe/Cu disorder to explain the magnetic properties of Cu-doped NaFeAs.

## ACKNOWLEDGMENTS

The DMFT model calculations of NaFeAs were supported by the state assignment of Minobrnauki of Russia

(theme “Electron” No. AAAA-A18-118020190098-5). The DFT+DMFT electronic structure calculations and magnetic properties analysis of NaFe<sub>0.5</sub>Cu<sub>0.5</sub>As were supported by the Russian Science Foundation (Project No. 19-12-00012).

- [1] E. Dagotto, *Rev. Mod. Phys.* **66**, 763 (1994); A. Damascelli, Z. Hussain, and Z.-X. Shen, *ibid.* **75**, 473 (2003); D. N. Basov and T. Timusk, *ibid.* **77**, 721 (2005); P. A. Lee, N. Nagaosa, and X.-G. Wen, *ibid.* **78**, 17 (2006); N. P. Armitage, P. Fournier, and R. L. Greene, *ibid.* **82**, 2421 (2010); B. Keimer, S. A. Kivelson, M. R. Norman, S. Uchida, and J. Zaanen, *Nature* **518**, 179 (2015).
- [2] M. V. Sadovskii, *Phys. Usp.* **51**, 1201 (2008); I. I. Mazin, *Nature* **464**, 183 (2010); J. Paglione and R. L. Greene, *Nat. Phys.* **6**, 645 (2010); G. R. Stewart, *Rev. Mod. Phys.* **83**, 1589 (2011); D. N. Basov and A. V. Chubukov, *Nat. Phys.* **7**, 272 (2011); P. Dai, J. Hu, and E. Dagotto, *ibid.* **8**, 709 (2012); P. C. Dai, *Rev. Mod. Phys.* **87**, 855 (2015); Q. Si, R. Yu, and E. Abrahams, *Nat. Rev. Mater.* **1**, 16017 (2016); R. M. Fernandes and A. V. Chubukov, *Rep. Prog. Phys.* **80**, 014503 (2017).
- [3] D. J. Scalapino, *Rev. Mod. Phys.* **84**, 1383 (2012).
- [4] R. M. Fernandes, A. V. Chubukov, and J. Schmalian, *Nat. Phys.* **10**, 97 (2014); J. K. Glasbrenner, I. I. Mazin, H. O. Jeschke, P. J. Hirschfeld, R. M. Fernandes, and R. Valentí, *ibid.* **11**, 953 (2015).
- [5] I. I. Mazin, D. J. Singh, M. D. Johannes, and M. H. Du, *Phys. Rev. Lett.* **101**, 057003 (2008); A. V. Chubukov, D. V. Efremov, and I. Eremin, *Phys. Rev. B* **78**, 134512 (2008); P. J. Hirschfeld, M. M. Korshunov, and I. I. Mazin, *Rep. Prog. Phys.* **74**, 124508 (2011); A. V. Chubukov, *Annu. Rev. Condens. Matter Phys.* **3**, 57 (2012).
- [6] P. J. Hirschfeld, D. Altenfeld, I. Eremin, and I. I. Mazin, *Phys. Rev. B* **92**, 184513 (2015); D. Altenfeld, P. J. Hirschfeld, I. I. Mazin, and I. Eremin, *ibid.* **97**, 054519 (2018).
- [7] P. O. Sprau, A. Kostin, A. Kreisel, A. E. Böhmer, V. Taufour, P. C. Canfield, S. Mukherjee, P. J. Hirschfeld, B. M. Andersen, and J. C. Séamus Davis, *Science* **357**, 75 (2017); A. Kostin, P. O. Sprau, A. Kreisel, Y. X. Chong, A. E. Böhmer, P. C. Canfield, P. J. Hirschfeld, B. M. Andersen, and J. C. Séamus Davis, *Nat. Mater.* **17**, 869 (2018).
- [8] C. C. Tsuei and J. R. Kirtley, *Rev. Mod. Phys.* **72**, 969 (2000).
- [9] Q. Si and E. Abrahams, *Phys. Rev. Lett.* **101**, 076401 (2008); M. M. Qazilbash, J. J. Hamlin, R. E. Baumbach, L. Zhang, D. J. Singh, M. B. Maple, and D. N. Basov, *Nat. Phys.* **5**, 647 (2009).
- [10] C. Weber, K. Haule, and G. Kotliar, *Nat. Phys.* **6**, 574 (2010).
- [11] T. Misawa, K. Nakamura, and M. Imada, *Phys. Rev. Lett.* **108**, 177007 (2012); R. Yu and Q. Si, *ibid.* **110**, 146402 (2013).
- [12] X. Deng, J. Mravlje, R. Zitko, M. Ferrero, G. Kotliar, and A. Georges, *Phys. Rev. Lett.* **110**, 086401 (2013).
- [13] L. de Medici, G. Giovannetti, and M. Capone, *Phys. Rev. Lett.* **112**, 177001 (2014).
- [14] R. Yu and Q. Si, *Phys. Rev. B* **84**, 235115 (2011).
- [15] S. Mandal, R. E. Cohen, and K. Haule, *Phys. Rev. B* **89**, 220502(R) (2014); I. Leonov, S. L. Skornyakov, V. I. Anisimov, and D. Vollhardt, *Phys. Rev. Lett.* **115**, 106402 (2015); S. L. Skornyakov, V. I. Anisimov, D. Vollhardt, and I. Leonov, *Phys. Rev. B* **96**, 035137 (2017); M. D. Watson, S. Backes, A. A. Haghghirad, M. Hoesch, T. K. Kim, A. I. Coldea, and R. Valentí, *ibid.* **95**, 081106(R) (2017); S. L. Skornyakov, V. I. Anisimov, D. Vollhardt, and I. Leonov, *ibid.* **97**, 115165 (2018); S. L. Skornyakov and I. Leonov, *ibid.* **100**, 235123 (2019).
- [16] M. Imada, A. Fujimori, and Y. Tokura, *Rev. Mod. Phys.* **70**, 1039 (1998).
- [17] E. M. Nica, R. Yu, and Q. Si, *npj Quant. Mater.* **2**, 24 (2017).
- [18] Y. Song, Z. Yamani, C. Cao, Y. Li, C. Zhang, J. S. Chen, Q. Huang, H. Wu, J. Tao, Y. Zhu, W. Tian, S. Chi, H. Cao, Y.-B. Huang, M. Dantz, T. Schmitt, R. Yu, A. H. Nevidomskyy, E. Morosan, Q. Si, and P. Dai, *Nat. Commun.* **7**, 13879 (2016).
- [19] A. F. Wang, J. J. Lin, P. Cheng, G. J. Ye, F. Chen, J. Q. Ma, X. F. Lu, B. Lei, X. G. Luo, and X. H. Chen, *Phys. Rev. B* **88**, 094516 (2013).
- [20] C. E. Matt, N. Xu, B. Lv, J. Ma, F. Bisti, J. Park, T. Shang, C. Cao, Yu Song, A. H. Nevidomskyy, P. Dai, L. Patthey, N. C. Plumb, M. Radovic, J. Mesot, and M. Shi, *Phys. Rev. Lett.* **117**, 097001 (2016).
- [21] C. Ye, W. Ruan, P. Cai, X. Li, A. Wang, X. Chen, and Y. Wang, *Phys. Rev. X* **5**, 021013 (2015).
- [22] J. D. Wright, T. Lancaster, I. Franke, A. J. Steele, J. S. Möller, M. J. Pitcher, A. J. Corkett, D. R. Parker, D. G. Free, F. L. Pratt, P. J. Baker, S. J. Clarke, and S. J. Blundell, *Phys. Rev. B* **85**, 054503 (2012).
- [23] J. T. Park, G. Friemel, T. Loew, V. Hinkov, Yuan Li, B. H. Min, D. L. Sun, A. Ivanov, A. Piovano, C. T. Lin, B. Keimer, and Y. S. Kwon, and D. S. Inosov, *Phys. Rev. B* **86**, 024437 (2012).
- [24] S. Li, C. de la Cruz, Q. Huang, G. F. Chen, T.-L. Xia, J. L. Luo, N. L. Wang, and P. Dai, *Phys. Rev. B* **80**, 020504(R) (2009).
- [25] C. Zhang, L. W. Harriger, Z. Yin, W. Lv, M. Wang, G. Tan, Y. Song, D. L. Abernathy, W. Tian, T. Egami, K. Haule, G. Kotliar, and P. Dai, *Phys. Rev. Lett.* **112**, 217202 (2014).
- [26] G. Tan, Y. Song, R. Zhang, L. Lin, Z. Xu, L. Tian, S. Chi, M. K. Graves-Brook, S. Li, and P. Dai, *Phys. Rev. B* **95**, 054501 (2017).
- [27] V. I. Anisimov, J. Zaanen, and O. K. Andersen, *Phys. Rev. B* **44**, 943 (1991); V. I. Anisimov, F. Aryasetiawan, and A. I. Lichtenstein, *J. Phys.: Condens. Matter* **9**, 767 (1997).
- [28] W. Metzner and D. Vollhardt, *Phys. Rev. Lett.* **62**, 324 (1989); A. Georges, G. Kotliar, W. Krauth, and M. J. Rozenberg, *Rev. Mod. Phys.* **68**, 13 (1996); V. I. Anisimov, A. I. Poteryaev, M. A. Korotin, A. O. Anokhin, and G. Kotliar, *J. Phys.: Condens. Matter* **9**, 7359 (1997); A. I. Lichtenstein and M. I. Katsnelson, *Phys. Rev. B* **57**, 6884 (1998); G. Kotliar, S. Y. Savrasov, K. Haule, V. S. Oudovenko, O. Parcollet, and C. A. Marianetti, *Rev. Mod. Phys.* **78**, 865 (2006); J. Kuneš, I. Leonov, P. Augustinský, V. Křápek, M. Kollar, and D. Vollhardt, *Eur. Phys. J. Spec. Top.* **226**, 2641 (2017); F. Nilsson and F. Aryasetiawan, *Computation* **6**, 26 (2018); P. R. C. Kent and G. Kotliar, *Science* **361**, 348 (2018).
- [29] A. Charnukha, Z. P. Yin, Y. Song, C. D. Cao, P. Dai, K. Haule, G. Kotliar, and D. N. Basov, *Phys. Rev. B* **96**, 195121 (2017).

- [30] Y. Xin, I. Stolt, Y. Song, P. Dai, and W. P. Halperin, *Phys. Rev. B* **101**, 064410 (2020).
- [31] K. Haule, J. H. Shim, and G. Kotliar, *Phys. Rev. Lett.* **100**, 226402 (2008); M. Aichhorn, L. Pourovskii, V. Vildosola, M. Ferrero, O. Parcollet, T. Miyake, A. Georges, and S. Biermann, *Phys. Rev. B* **80**, 085101 (2009); S. L. Skornyakov, A. A. Katanin, and V. I. Anisimov, *Phys. Rev. Lett.* **106**, 047007 (2011); S. L. Skornyakov, V. I. Anisimov, and D. Vollhardt, *Phys. Rev. B* **86**, 125124 (2012); M. Aichhorn, L. Pourovskii, and A. Georges, *ibid.* **84**, 054529 (2011); J. M. Tomczak, M. van Schilfhaarde, and G. Kotliar, *Phys. Rev. Lett.* **109**, 237010 (2012); Z. P. Yin, K. Haule, and G. Kotliar, *Phys. Rev. B* **86**, 195141 (2012); P. Werner, M. Casula, T. Miyake, F. Aryasetiawan, A. J. Millis, and S. Biermann, *Nat. Phys.* **8**, 331 (2012); A. Georges, L. de' Medici, and J. Mravlje, *Annu. Rev. Condens. Matter Phys.* **4**, 137 (2013); M. Hirayama, T. Miyake, and M. Imada, *Phys. Rev. B* **87**, 195144 (2013); I. A. Nekrasov, N. S. Pavlov, and M. V. Sadovskii, *JETP Lett.* **102**, 26 (2015); A. van Roekeghem, L. Vaugier, H. Jiang, and S. Biermann, *Phys. Rev. B* **94**, 125147 (2016).
- [32] Z. P. Yin, K. Haule, and G. Kotliar, *Nat. Phys.* **7**, 294 (2011); *Nat. Mater.* **10**, 932 (2011).
- [33] N. Marzari, A. A. Mostofi, J. R. Yates, I. Souza, and D. Vanderbilt, *Rev. Mod. Phys.* **84**, 1419 (2012); V. I. Anisimov, D. E. Kondakov, A. V. Kozhevnikov, I. A. Nekrasov *et al.*, *Phys. Rev. B* **71**, 125119 (2005); D. Korotin, A. V. Kozhevnikov, S. L. Skornyakov, I. Leonov, N. Binggeli, V. I. Anisimov, and G. Trimarchi, *Eur. Phys. J. B* **65**, 91 (2008); G. Trimarchi, I. Leonov, N. Binggeli, Dm. Korotin, and V. I. Anisimov, *J. Phys.: Condens. Matter* **20**, 135227 (2008).
- [34] I. Leonov, V. I. Anisimov, and D. Vollhardt, *Phys. Rev. B* **91**, 195115 (2015).
- [35] L. V. Pourovskii, B. Amadon, S. Biermann, and A. Georges, *Phys. Rev. B* **76**, 235101 (2007); B. Amadon, F. Lechermann, A. Georges, F. Jollet, T. O. Wehling, and A. I. Lichtenstein, *ibid.* **77**, 205112 (2008).
- [36] I. Leonov, N. Binggeli, Dm. Korotin, V. I. Anisimov, N. Stojić, and D. Vollhardt, *Phys. Rev. Lett.* **101**, 096405 (2008); I. Leonov, Dm. Korotin, N. Binggeli, V. I. Anisimov, and D. Vollhardt, *Phys. Rev. B* **81**, 075109 (2010); I. Leonov, *ibid.* **92**, 085142 (2015); I. Leonov, L. Pourovskii, A. Georges, and I. A. Abrikosov, *ibid.* **94**, 155135 (2016); I. Leonov, A. O. Shorikov, V. I. Anisimov, and I. A. Abrikosov, *ibid.* **101**, 245144 (2020).
- [37] S. Baroni, S. de Gironcoli, A. Dal Corso, and P. Giannozzi, *Rev. Mod. Phys.* **73**, 515 (2001); P. Giannozzi, S. Baroni, N. Bonini, M. Calandra, R. Car *et al.*, *J. Phys.: Condens. Matter* **21**, 395502 (2009).
- [38] P. Werner, A. Comanac, L. de Medici, M. Troyer, and A. J. Millis, *Phys. Rev. Lett.* **97**, 076405 (2006); E. Gull, A. J. Millis, A. I. Lichtenstein, A. N. Rubtsov, M. Troyer, and P. Werner, *Rev. Mod. Phys.* **83**, 349 (2011).
- [39] H. J. Vidberg and J. W. Serene, *J. Low Temp. Phys.* **29**, 179 (1977).
- [40] R. Yu and Q. Si, *Phys. Rev. B* **96**, 125110 (2017).
- [41] W. F. Brinkman and T. M. Rice, *Phys. Rev. B* **2**, 4302 (1970).
- [42] T. J. Liu, J. Hu, B. Qian, D. Fobes, Z. Q. Mao, W. Bao, M. Reehuis, S. A. J. Kimber, K. Prokeš, S. Matas, D. N. Argyriou, A. Hiess, A. Rotaru, H. Pham, L. Spinu, Y. Qiu, V. Thampy, A. T. Savici, J. A. Rodriguez, and C. Broholm, *Nat. Mater.* **9**, 718 (2010); G. S. Tucker, D. K. Pratt, M. G. Kim, S. Ran, A. Thaler, G. E. Granroth, K. Marty, W. Tian, J. L. Zarestky, M. D. Lumsden, S. L. Bud'ko, P. C. Canfield, A. Kreyssig, A. I. Goldman, and R. J. McQueeney, *Phys. Rev. B* **86**, 020503(R) (2012); Y. Texier, Y. Laplace, P. Mendels, J. T. Park, G. Friemel, D. L. Sun, D. S. Inosov, C. T. Lin, and J. Bobroff, *Europhys. Lett.* **99**, 17002 (2012); R. M. Fernandes and A. J. Millis, *Phys. Rev. Lett.* **110**, 117004 (2013).
- [43] A. I. Lichtenstein, M. I. Katsnelson, V. P. Antropov, and V. A. Gubanov, *J. Magn. Magn. Mater.* **67**, 65 (1987); Y. O. Kvashnin, O. Grånäs, I. Di Marco, M. I. Katsnelson, A. I. Lichtenstein, and O. Eriksson, *Phys. Rev. B* **91**, 125133 (2015); D. M. Korotin, V. V. Mazurenko, V. I. Anisimov, and S. V. Streltsov, *ibid.* **91**, 224405 (2015).
- [44] S. Mandal, K. Haule, K. M. Rabe, and D. Vanderbilt, *Phys. Rev. B* **100**, 245109 (2019).
- [45] Y. Xin, I. Stolt, J. A. Lee, Y. Song, P. Dai, and W. P. Halperin, *Phys. Rev. B* **99**, 155114 (2019).
- [46] Here we use the following notation for the Heisenberg model  $H = \sum_{i>j} J_{ij} \mathbf{S}_i \cdot \mathbf{S}_j$ .
- [47] M. J. Han, Q. Yin, W. E. Pickett, and S. Y. Savrasov, *Phys. Rev. Lett.* **102**, 107003 (2009).